INVESTIGATION OF EFFECT OF ENERGY DISSIPATION BEHIND A DETACHED SHOCK WAVE ON TOTAL HEAD MEASUREMENTS

Thesis

by

Basil Staros

In Partial Fulfillment of the Requirements for the Degree of

Aeronautical Engineer

California Institute of Technology

Pasadena, California

1950

ACKNOWLEDGMENTS

The author wishes to express his appreciation to Professor H. J. Stewart for his constant help and guidance during the course of the work. Sincere thanks are also due Dr. Allen E. Puckett for his suggestions and assistance in the initial formulation of the problem, and Miss Louise Iarussi and Mrs. Mary Arthur for their assistance in the preparation of the manuscript.

ABSTRACT

The flow field behind a detached shock wave, created by a blunt body in a supersonic air stream, is analyzed with respect to energy dissipation through the action of viscosity in the fluid stress field near the axis of symmetry. This energy dissipation is related to the rise in entropy, and consequently to the additional drop in reservoir pressure beyond that given by the Rayleigh pitot tube formula. The method is applied to the calculations of an apparent defect in reservoir pressure, for more precise calculations of free stream Mach numbers using total head tube measurements.

TABLE OF CONTENTS

TABLE OF FIGURES

SYMBOLS

a - radius of pitot tube at nose

c - speed of sound

c_p - specific heat at constant pressure

$f(\ )$ - function of

h - wedge stagger

K_1 - constant defined by Equation (24)

K_2 - constant defined by Equation (25)

L - parameter, reduced entropy level at $x = \delta$

η - parameter defined by Equation (19)

M - Mach number

p - pressure

Q - rate of inflow of heat per unit volume due to thermal conductivity

R - gas constant

Re - Reynolds number, defined by Equation (22)

Δs - change in entropy

t - boundary layer thickness at stagnation point

T - temperature

u - velocity in x direction

U - velocity at infinity, potential solution

v - velocity in y direction

w - velocity in z direction

xyz - coordinates, orthogonal axes

β_o - angle of shock wave to free stream flow direction

β - parameter, boundary layer problem

γ - ratio of specific heats $c_p/c_v = 1.40$

δ - distance of detachment of shock from nose of pitot tube

ϵ - location of stagnation point for potential solution

η - parameter in boundary layer problem

θ - wedge half angle

λ - coefficient of thermal conductivity

μ - coefficient of viscosity

ν - kinematic viscosity = μ/ρ

ρ - density

σ - Prandtl number = $\frac{\mu c_p}{\lambda}$

Φ - dissipation function, defined on page 11

$( )_o$ - reservoir conditions

$( )_1$ - free stream condition

$( )_2$ - free stream conditions after normal shock

$( )_o'$ - reservoir conditions after normal shock

$( )_o''$ - reservoir conditions at nose of pitot tube

I. INTRODUCTION

A. General

The most direct method for determining the state of a fluid at some arbitrary point requires knowledge of three fundamental flow parameters, which may be, for instance, pressure, temperature, and velocity. Therefore, three items of data must be available. However, it is possible to determine one or two of these parameters at some point in the fluid other than the one for which a complete description of the state of the fluid is desired. This possibility is dependent on the availability of this supplementary information, and on the existence of a relationship, in a convenient form, between the state parameters for these two points.

In a subsonic wind tunnel, the local reservoir pressure and temperature, except in the boundary layer, are assumed to be equal to the pressure and temperature that actually exist in the reservoir. This assumption implies a condition of isentropy for the entire flow. The static pressure may be determined by a local measurement at the wall without disturbing the flow, and assumed constant across the section of the tunnel. Thus, applying the condition of isentropy, the local Mach number, or velocity, may be determined from the following relations:

$$\frac{p}{p_o} = \left(1 + \frac{\gamma-1}{2} M^2\right)^{-\frac{\gamma}{\gamma-1}} \qquad (1a)$$

$$c = \sqrt{\gamma R T} \tag{1b}$$

$$\frac{T}{T_o} = 1 + \frac{\gamma - 1}{2} M_1^2 \tag{1c}$$

$$u_1 = M_1 c \tag{1d}$$

If the local stagnation pressure is not known, owing to entropy changes along the channel either by cooling or by dissipation in a boundary layer, an additional measurement must be made. A total head, or pitot tube, serves for this purpose. However, here it is assumed that the flow decelerates isentropically to the stagnation point of the tube. In this case, the local conditions may again be determined from the relations above.

If the flow velocity is greater than a Mach number of 1.0, these same relations are applicable. However, if the local stagnation pressure is not known, the determination of this pressure is not as convenient as in the subsonic case. The deceleration to the nose of the total head tube is not isentropic, for a detached shock wave must form in front of the tube. Immediately in front of the stagnation point of this body the shock wave is normal to the axis of the body; consequently, the fluid can be treated as if it actually traversed a normal shock. Applying the known relations for the change in the total head across a normal shock, and further assuming that the flow behind the shock can again be treated as an isentropic phenomenon, the local

reservoir pressures in the fluid before and after the detached shock are related by the following expression:

$$\frac{p_o}{p_{o'}} = \left(\frac{2\gamma}{\gamma+1} M_1^2 - \frac{\gamma-1}{\gamma+1}\right)^{\frac{1}{\gamma-1}} \left[\frac{1 + \frac{\gamma-1}{2} M_1^2}{\frac{\gamma+1}{2} M_1^2}\right]^{\frac{\gamma}{\gamma-1}} \qquad (2)$$

From the relation between p_o and p given above, the Rayleigh pitot formula is directly deducible.

$$\frac{p}{p_{o'}} = \frac{\left(\frac{2\gamma}{\gamma+1} M_1^2 - \frac{\gamma-1}{\gamma+1}\right)^{\frac{1}{\gamma-1}}}{\left(\frac{\gamma+1}{2} M_1^2\right)^{\frac{\gamma}{\gamma-1}}} \qquad (3)$$

If the local static and pitot total head pressures are known, the Mach number can be determined from Equation (3).

B. Mach Number Determination in a Supersonic Wind Tunnel

There exist four direct and relatively accurate methods by which it is possible to make a fairly accurate determination of the Mach number in the test section of a supersonic wind tunnel.

The first method is the simplest, requiring no more than a measurement of the reservoir pressure and a measurement of the static pressure with an orifice located at a convenient point in the wall of the test section. The Mach number can be determined from Equation (1a). For high precision, or for complete axial surveys of the variation of Mach number along the center line of the test section, this simple procedure is not very useful.

The second method is actually a refinement of the first. The reservoir pressure is measured as before; however, the static pressure is now measured at orifices located on both sides of a sharp wedge of small total included angle. Adjustment of the wedge in pitch to zero the difference between the

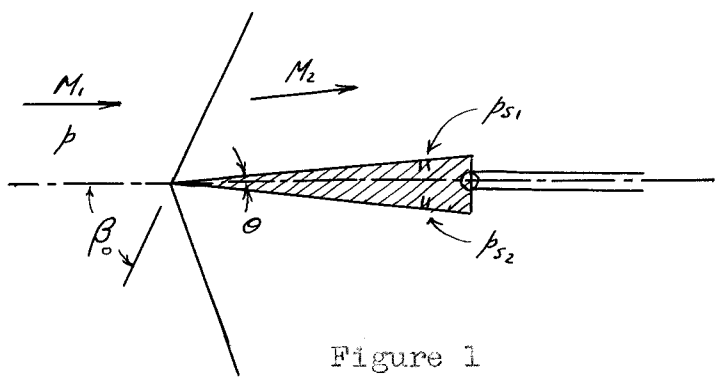

Figure 1

Single Wedge Method for Determination of Free Stream Mach Number

two static pressures p_{s_1} and p_{s_2} guarantees a flow direction parallel to the axis of wedge, and assures a change in flow direction for either side to equal the half angle of the wedge. Assuming isentropic flow everywhere, except across the oblique shock, the true Mach number ahead of the shock wave can be determined from the following oblique shock relations:

$$\frac{p_{s_1}}{p} = \frac{2\gamma}{\gamma+1} M_1^2 \sin^2\beta_o - \frac{\gamma-1}{\gamma+1} \tag{4}$$

$$\frac{1}{M_1^2} = \sin^2\beta_o - \frac{\gamma+1}{2} \frac{\sin\beta_o \cos\theta}{\cos(\beta_o-\theta)} \tag{5}$$

and the isentropic channel pressure relation expressed in Equation (1a).

For specific values of p_o, θ, and p_{s_1}, it is possible to determine p, M_1, and β_o. This method has the additional advantage of making possible a complete survey of pressure and Mach number continuously along any line parallel to the center line of the tunnel, throughout the entire test section. The method is still applicable if the wedge is not adjustable in pitch; here, however, the interpretation of data is a little more lengthy.

The third method is more elaborate. In addition to the wedge of the previous method, an additional fixed wedge (II) is mounted in the tunnel just above and downstream of the first wedge (I), and arranged such that the

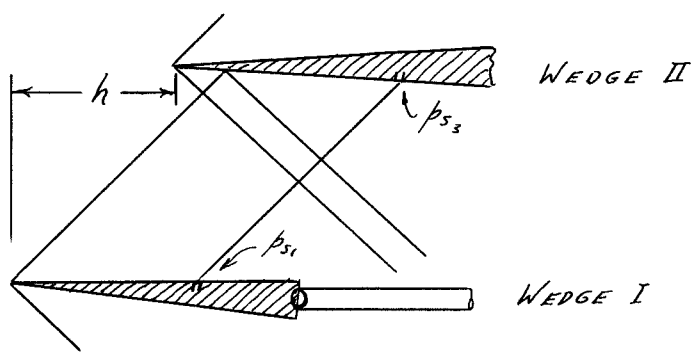

Figure 2

Double Wedge Method for Determination of Free Stream Mach Number

stagger (h) and angle of pitch of wedge (I) are both independentally adjustable. An initial determination of p_{s_3} is made when the entire disturbance caused by wedge (I) lies completely downstream from the p_{s_3} orifice. Wedge (I), with the upper surface approximately parallel to the flow, is then moved axially upstream until the orifice p_{s_1} lies on the character-

istic of the orifice p_{s_3}. This position is determined by observing the point where the orifice p_{s_1}, connected to a high vacuum, has the maximum effect on the value of p_{s_3}. The value of p_{s_1}, after wedge (I) is pitched until p_{s_3} agrees with the initial determination of p_{s_3}, is then the free stream static pressure. The measurement is actually made behind a double family of Mach waves and expansion waves created by the boundary layer along the upper surface of the wedge. The cumulative effect of these waves is sensibly zero, as indicated by the return of p_{s_3} to its original value. Again, the Mach number may be quickly determined by Equation (1a).

The fourth method is simply a determination of the total head behind a detached shock wave. By directly applying the Rayleigh pitot tube formula, the Mach number can be determined.

C. Experimental Evidence

In the calibration of the 12-inch supersonic wind tunnel at the Jet Propulsion Laboratory, the single static wedge method was used for Mach number surveys. However, both the double wedge method and the total head tube method were employed as checks on the primary method. Very good agreement between the two static wedge methods was observed at M = 2.174, and a minor departure from

this value (M = 2.176), not creditable to lack of instrument precision, was observed for the total head tube method. The observed data indicated an apparent defect in p_o', as measured by the total head tube.

At higher Mach numbers, there is evidence that the disagreement is more pronounced.

The fundamental objective of this thesis is to investigate the effect of energy dissipation behind the detached shock wave as the cause for this discrepancy, and to determine the order of magnitude of this effect in supersonic total head measurements.

II. INVESTIGATION OF ENTROPY RISE BEHIND A DETACHED SHOCK WAVE

A. Technique and Assumptions

For pitot tubes, or other blunt bodies of revolution in a supersonic flow, the distances of detachment of the shock waves are usually very small. This is especially true for very high Mach numbers. Figure 5, extracted from Reference (1), illustrates the variation of this distance with Mach number, as measured in experimental programs. Within the detachment span, the flow must adjust from the conditions which prevail immediately downstream from the detached shock to the conditions which prevail on the surface of the body. This action indicates that for sufficiently high supersonic velocities the flow field in this region is characterized by large velocity stresses. If the viscosity of the fluid is not zero, energy dissipation may account for an apparent defect in p_o'.

In the vicinity of the axis of symmetry, the region within the detachment span is separated into two zones, depending on the role of viscosity in determining the character of the flow. The upstream zone is considered to possess the potential type flow pattern of a fluid without viscosity. In this zone the flow velocity along the axis of symmetry is constructed to match the velocity

of the fluid immediately downstream from a normal shock wave, at the detachment distance δ from the nose of the body. In this zone, the subsequent introduction of viscosity is considered to produce a negligible effect on the velocity pattern given by the potential solution, such that, to a first approximation, the dissipation of energy throughout this zone can be conveniently obtained. This is effectively the first step of an iteration procedure to obtain the exact nature of the flow in a region where the viscosity is sufficiently low to account for only a small perturbation on the flow field as determined for a perfect fluid.

The downstream zone is the boundary layer on the nose of the body. The boundary layer thickness is defined to be that distance from the nose of the body where the effect of viscosity in shaping the form of the flow becomes negligibly small. For this application, it is considered to be that distance beyond which the velocity gradient along the axis of symmetry, as given by the boundary layer solution, approaches a constant within 0.1%. At this distance, the parameter included in the boundary layer problem can be adjusted to provide the matching of velocities of the potential solution to that of the boundary layer solution. Since the potential solution of the upstream part is constructed under the assumption of zero viscosity, while the

boundary layer solution considers a finite viscosity for all of the fluid, it is impossible to provide a matching of both the velocity and the velocity gradient at a common point. However, a matching of the velocity gradients together with the velocities can occur at two different points, one pertaining to the potential solution and the other to the boundary layer solution. This can be interpreted as a virtual increase in the radius of the body, amounting to the distance between these points, in the construction of the potential solution.

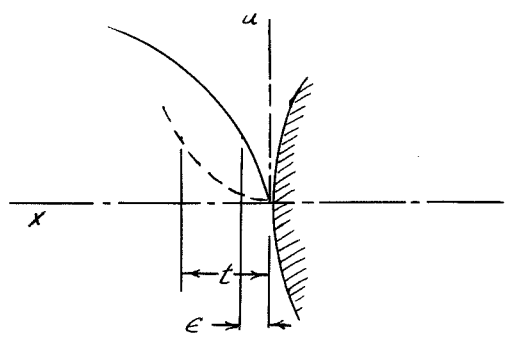

Figure 3

Axial Velocity Profile in Region of Nose of Pitot Tube for both Potential and Boundary Layer Solutions

The change in entropy for an adiabatic process is given by

$$T \frac{Ds}{Dt} = \frac{1}{\rho} \Phi + \frac{1}{\rho} \frac{DQ}{Dt} \qquad (6)$$

where

$$\frac{D}{Dt} = \frac{\partial}{\partial t} + u \frac{\partial}{\partial x} + v \frac{\partial}{\partial y} + w \frac{\partial}{\partial z}$$

and where ϕ, the dissipation function, is given by

$$\phi = -\frac{2}{3}\mu\left[\frac{du}{dx} + \frac{dv}{dy} + \frac{dw}{dz}\right]^2 + 2\mu\left[\left(\frac{du}{dx}\right)^2 + \left(\frac{dv}{dy}\right)^2 + \left(\frac{dw}{dz}\right)^2\right]$$
$$+ \mu\left[\frac{dv}{dx} + \frac{du}{dy}\right]^2 + \mu\left[\frac{dw}{dy} + \frac{dv}{dz}\right] + \mu\left[\frac{du}{dz} + \frac{dw}{dx}\right]^2$$

See Reference (2), article 358. Q represents the rate of inflow of heat per unit volume due to thermal conductivity.

In the vicinity of the axis of symmetry, all velocities and velocity gradients, except u and $\frac{du}{dx}$, are taken to be zero. Also, all temperature gradients, except $\frac{dT}{dx}$, are assumed zero. This is inferred from the symmetrical character of the flow in this region.

Equation (6) then reduces, for steady state flow, to

$$u\,T\,\frac{ds}{dx} = \nu\frac{4}{3}\left(\frac{du}{dx}\right)^2 + \frac{1}{\rho}\frac{d}{dx}\left(\lambda\frac{dT}{dx}\right) \qquad (6a)$$

where λ is the coefficient of thermal conductivity. Assuming λ constant and also assuming that

$$\sigma = \frac{\mu C_p}{\lambda} = 1 \qquad \text{(Prandtl number)}$$

Equation (6a) can be written in either of the two following forms:

$$u\,T\,\frac{ds}{dx} = \nu\frac{4}{3}\left(\frac{du}{dx}\right)^2 + \frac{\lambda}{\rho}\frac{d^2T}{dx^2}$$
$$= \nu\frac{4}{3}\left(\frac{du}{dx}\right)^2 - \nu\left[u\frac{d^2u}{dx^2} + \left(\frac{du}{dx}\right)^2\right] \qquad (7)$$

The second form of Equation (7) follows for no heat transfer through the body.

From this, it appears that the effect of conductivity may be of the same order of magnitude as the effect of viscous dissipation. Since no simple integral of the boundary layer equations (corresponding to Appendix A) is known which considers the effect of heat transfer, it is not possible to carry out the complete solution; consequently the effects of heat transfer will be neglected in these calculations.

Neglecting variation in T and ν and neglecting the heat transfer terms, Equation (7) becomes

$$\Delta S = \frac{4\nu}{3T} \int_0^\delta \frac{1}{a} \left(\frac{du}{dx}\right)^2 dx \qquad (8)$$

Using the velocity and velocity gradients as determined by the method described above, the entropy change through the detachment span can be evaluated. From this change the drop in reservoir pressure can be determined, using

$$\Delta S = R \log \frac{p_o'}{p_o''} \qquad (9)$$

For $\Delta S \ll R$, this equation reduces to

$$\frac{p_o'}{p_o} = 1 + \frac{\Delta S}{R} \qquad (9a)$$

The change in entropy through the detachment span will obviously be a function of the free stream Mach number M_1. Consequently, in line with the assumption that the change in entropy is small, the approximation that $p_o'' = p_o'$ and the

application of the Rayleigh pitot formula (Eq. 3) allow the determination of an uncorrected M_1 for use in evaluating ΔS, and subsequently lead to the evaluation of a corrected M_1 through Equation (9a).

B. Matching Potential and Boundary Layer Solutions

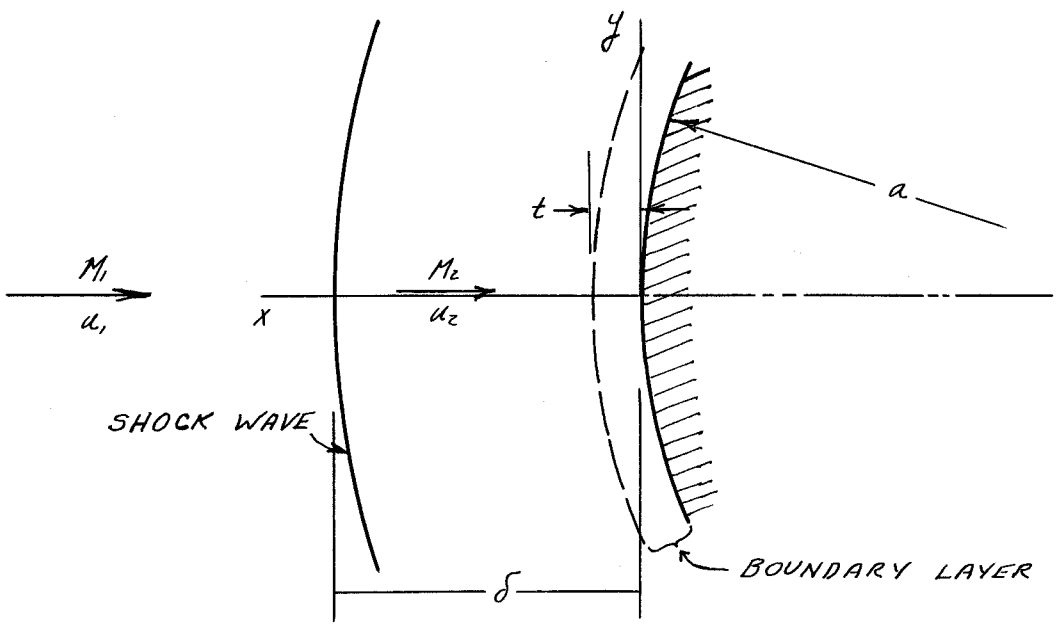

Figure 4

Sketch of Flow Geometry in Region of Nose of Pitot Tube

In accordance with the definition given in Section A for the boundary layer thickness, from Appendix A

$$\eta = 2.00$$

$$t = 2\left(\frac{\nu}{\beta}\right)^{\frac{1}{2}} \qquad (10)$$

Hence, at $x = t$

$$u_2 = -2.90\,(\beta\nu)^{\frac{1}{2}}$$

$$\frac{du_2}{dx} = -2\beta$$

From the potential solution for the region outside the boundary layer, the velocity and the velocity gradient along the axis of symmetry are

$$u_2 = -U + U\,\frac{a^3}{(x+a)^3}$$

$$\frac{du_2}{dx} = -3U\,\frac{a^3}{(x+a)^4}$$

where $-U$ is the velocity at infinity for the potential flow. At $x = \epsilon$

$$u_2 = -U + U\,\frac{a^3}{(\epsilon+a)^3}$$

$$\frac{du_2}{dx} = -3U\,\frac{a^3}{(\epsilon+a)^4}$$

Equating velocities and velocity gradients at these points,

$$-2.90\,(\beta\nu)^{\frac{1}{2}} = -U + U\,\frac{a^3}{(\epsilon+a)^3}$$

$$-2\beta = 3U\,\frac{a^3}{(\epsilon+a)^4}$$

from which β and ϵ can be determined. Assuming $\epsilon/a < 1$,

$$\beta = \frac{3}{2}\,\frac{U}{a}\left(1 + 2\frac{\epsilon}{a} + O\left(\frac{\epsilon}{a}\right)^2\right) \qquad (11)$$

$$\epsilon \cong 0.73\, t = 1.45 \left(\frac{\nu}{\beta}\right)^{\frac{1}{2}} \qquad (12)$$

At $x = \delta - \epsilon$, the velocity along the axis of symmetry in the potential solution is matched to the velocity of the fluid immediately downstream from the detached shock wave. Thus U can be expressed in terms of the detachment distance δ, the radius of the tube, and the free stream velocity.

$$-u_2 = -U + U\left[1 - 3\frac{\delta-\epsilon}{a} + O\left(\frac{\delta-\epsilon}{a}\right)^2\right]$$

$$U^2\left(\frac{3\delta}{a}\right)^2 - \left(2u_2\frac{3\delta}{a} + 12.6\frac{\nu}{a}\right)U + u_2^2 = 0$$

Since for most practical cases

$$u_2\frac{\delta}{a} > \frac{\nu}{a}$$

the second factor of U can be neglected, leaving

$$U = u_2\frac{a}{3\delta} \qquad (13)$$

From the basic equation for the velocity change across a normal shock wave

$$u_1 u_2 = c^{*2}$$

$$u_2 = \frac{c_0}{M_1}\frac{2}{\gamma+1}\left(1 + \frac{\gamma-1}{2}M_1^2\right)^{\frac{1}{2}}$$

Thus

$$U = \frac{c_0}{3(\gamma+1)\,\delta/a}\,\frac{2}{M_1}\left(1+\frac{\gamma-1}{2}M_1^2\right)^{\frac{1}{2}} \qquad (14)$$

For $M_1 > 3$, δ/a approaches 0.14 with negligible variation in this value for higher Mach numbers. See Figure 5. With this restriction, Equation (13) can be written

$$U = \frac{2\,c_0}{M_1}\left(1+\frac{\gamma-1}{2}M_1^2\right)^{\frac{1}{2}} \qquad (15)$$

C. Solution for Entropy Rise, Using Potential Form for Velocity Distribution

The entropy change through the detachment span, except for the boundary layer, can be determined from Equation (8)

$$\Delta S = \frac{4\nu_0'}{3T_0'}\int_{\delta}^{\epsilon}\frac{1}{u_2}\left(\frac{du_2}{dx}\right)^2 dx$$

where, from potential form of velocity pattern,

$$u_2 = U\frac{a^3}{(x+a)^3} - U$$

$$\frac{du_2}{dx} = -U\frac{3a^3}{(x+a)^4}$$

The integral can then be simply evaluated.

$$\Delta S = \frac{12\,\nu_0'\,U}{T_0'\,a}\left[-\frac{1}{4(1+\frac{x}{a})^4} - \frac{1}{(1+\frac{x}{a})} + \frac{1}{6}\log\left(1+\frac{3}{x/a}+\frac{3}{(x/a)^2}\right) + \frac{\sqrt{3}}{3}\tan^{-1}\left(-\frac{2\sqrt{3}}{3}\,\frac{x}{a}-\sqrt{3}\right)\right]_{\delta}^{\epsilon}$$

Figure 6 is a plot of the value of this expression as a function of δ/a . For

$$\epsilon = 1.45 \left(\frac{\nu_0'}{\beta}\right)^{\frac{1}{2}} \tag{12}$$

$$\beta = \frac{2}{2} \frac{U}{a} \tag{11}$$

the change in entropy across this portion of the detachment span can be expressed in the form

$$\Delta S = \frac{12\,\nu_0'\,U}{T_0'\,a}\left[\frac{1}{6}\log\left(2.14\,\frac{aU}{\nu'}\right) - 1.855 - L\right] \tag{16}$$

where

$$\frac{12\,\nu_0'\,U}{T_0'\,a}\,L$$

represents the value of the integral at $x = \delta$.

D. Solution for Entropy Rise Through Boundary Layer

The entropy change through the boundary layer can be evaluated in two ways. The simplest method, and perhaps in practice the most accurate method, is to integrate stepwise, using the tabulated data from the boundary layer solution. The other method is to choose enough terms of the series solution for the velocity in the boundary layer to provide an accurate representation of this velocity, and then integrate as before, using Equation (8). If two terms are selected, then

$$u_2 = -1.3172 \left(\frac{\beta}{\nu}\right)^{\frac{1}{2}} \beta x^2 + 0.3333 \frac{\beta}{\nu} \beta x^3$$

$$\frac{du_2}{dx} = -2.6344 \left(\frac{\beta}{\nu}\right)^{\frac{1}{2}} \beta x + \frac{\beta}{\nu} \beta x^2$$

as given in Appendix A. Substitution into Equation (8) with proper limits

$$\Delta S = \frac{4 \nu_0'}{3 T_0'} \int_t^0 \frac{1}{u_2} \left(\frac{du_2}{dx}\right)^2 dx$$

where

$$t = 2 \left(\frac{\nu_0'}{\beta}\right)^{\frac{1}{2}}$$

$$\beta = \frac{3}{2} \frac{U}{a}$$

The result is, after the integration is carried out,

$$\Delta S = 11.15 \frac{\nu_0' U}{T_0' a}$$

To integrate stepwise, Equation (8) written in terms of the boundary layer solution nomenclature becomes

$$\Delta S = \frac{8 \nu_0' \beta}{3 T_0'} \int_0^2 \frac{[f'(\eta)]^2}{f(\eta)} d\eta$$

Evaluating from data in Appendix A, the result is

$$\Delta S = 12 \frac{\nu_0' U}{T_0' a} \qquad (17)$$

The evaluation of the change in entropy using the two term approximation for the boundary layer velocity agrees fairly well with this value.

E. Total Entropy Rise Equation

The total change in entropy through the entire detachment span is then the sum of the entropy changes given by Equations (16) and (17).

$$\Delta S = \frac{12\,\nu_o'\,U}{T_o'\,a}\left[\frac{1}{6}\log 2.14\,\frac{a\,U}{\nu_o'} - 0.855 - L\right] \qquad (18)$$

To reduce Equation (18) to a simple usable relation, Equation (14) is rewritten as

$$U = c_o\,\eta$$

where

$$\eta = \frac{1}{3(\gamma+1)\,\delta/a}\,\frac{2}{M_1}\left(1 + \frac{\gamma-1}{2}M_1^2\right)^{\frac{1}{2}} \qquad (19)$$

In addition, since $T_o' = T_o$ within the approximation of constant T_o' throughout the entire detachment span, the kinematic viscosity within the detachment span can be approximated by

$$\nu_o' = \nu_o\,\frac{\rho_o}{\rho_o'} \qquad (20)$$

where ν_o is the kinematic viscosity based upon reservoir conditions. This assumption is valid for the entire detachment span provided that

$$\frac{\rho_o'}{\rho_o''} \cong 1 \qquad (21)$$

which is in line with the assumption that the entropy change through the detachment span is small, and also provided that

$$\nu_0' = \nu_0''$$

Letting

$$Re = \frac{a\, c_0}{\nu_0} \tag{22}$$

represent a Reynolds number based upon the radius of the pitot tube head, the reservoir speed of sound, and the reservoir kinematic viscosity, Equation (18) then reduces to

$$\Delta S = \frac{4822}{Re}\left(\eta \frac{p_0}{p_0'}\right)\left[\log Re + \log \eta \frac{p_0'}{p_0} - 4.37 - 6L\right] \tag{23}$$

Defining

$$K_1 = \eta \frac{p_0}{p_0'} \tag{24}$$

$$K_2 = \log \eta \frac{p_0'}{p_0} - 4.37 - 6L \tag{25}$$

both of which are functions of the Mach number, Equation (23) can be written

$$\Delta S = \frac{4822\, K_1}{Re}\left[\log Re + K_2\right] \tag{26}$$

From Equation (9a), continuing the assumption of Equation (21)

$$\frac{p_o'}{p_o''} = 1 + \frac{2.81\,K_1}{Re}\left[\log Re + K_2\right] \qquad (27)$$

The parameters K_1 and K_2 are plotted against M_1 in Figures 7 and 8. The values of δ/a used in the evaluation of these parameters as a function of Mach number are selected from the curve drawn in Figure 5.

III. RESULTS

To provide some measure for evaluating the significance of Equation (27) in predicting the drop in reservoir pressure ratio across the detachment span, several computations were made based upon assumed initial conditions. The results are as follows:

Case I

T_o = 540 ° Rankine
p_o = 93.3 lb./sq. in. absol.
ρ_o = 0.0145 slugs/cubic ft.
a = 0.0117 feet
M_1 = 1.70

whereupon

Re = 5.0×10^5
ΔS = 0.10 ft^2/sec^2 °Rankine
p_o'/p_o'' = 1.000063
M_1 = 1.70

The values selected here for initial conditions agree with those specified in Appendix B, or Reference (5). The step integration technique employed in Appendix B yielded the values

ΔS = 0.086 ft^2/sec^2 °Rankine
p_o'/p_o'' = 1.000050
M_1 = 1.70

These two results are in fair agreement. However, it is to be noted that if corrections were made to the values of K_1 and K_2, which are strictly necessary owing to the lack of correspondence in the value of δ/a used in their evaluation to that of Appendix B, the results by the theoretical approach of Equations (26) and (27) become

$$\Delta S = 0.086 \quad ft^2/sec^2 \, ^\circ Rankine$$
$$p_o'/p_o'' = 1.000050$$
$$M_1 = 1.70$$

The agreement is then very good.

Case II

Using the same initial conditions of Case I except that now $M_1 = 9.00$,

$$Re = 5.0 \times 10^5$$
$$\Delta S = 14.4 \quad ft^2/sec^2 \, ^\circ Rankine$$
$$p_o'/p_o'' = 1.0084$$
$$M_1 = 9.017$$

Case III

Using the same initial conditions of Case II, except that now the radius of the tube end is reduced by a factor of 5,

$$Re = 1.0 \times 10^5$$
$$\Delta S = 57.6 \quad ft^2/sec^2 \, ^\circ Rankine$$
$$p_o'/p_o'' = 1.0336$$
$$M_1 = 9.067$$

IV. CONCLUSIONS

The results of this investigation indicate that the energy dissipation in the flow field behind a detached shock wave, created by a blunt body in a supersonic air stream, is quite small and produces only a minor change of the reservoir pressure at the stagnation point from the reservoir pressure existing immediately downstream from the detached shock wave. This condition is especially true for the majority of cases where the Mach number is only moderately high (around $M_1 = 5$ or 6, or less), and the Pitot tubes are of average dimensions ($a = 0.125$ inch or greater). Here the errors obtained in the computation of the true Mach number M_1 are well beyond experimental observation in ordinary engineering applications. This investigation consequently does not explain the apparent defect in p_o' experienced in the calibration of the 12-inch supersonic wind tunnel at the Jet Propulsion Laboratory, as mentioned in Section I-C.

For very high Mach numbers, and for small pitot tubes, this investigation indicates that the dissipation of energy within the detachment span may account for a small but measurable error in the determination of the true free stream Mach number. For experiments demanding a high degree of precision, the effect should be taken into account.

REFERENCES

(1) Henry T. Nagamatsu, "Theoretical Investigation of Detached Shock Wave", Thesis, California Institute of Technology (1949).

(2) Horace Lamb, "Hydrodynamics", Cambridge University Press, 1932.

(3) S. Goldstein, "Modern Developments in Fluid Dynamics", Oxford University Press, 1938.

(4) Von F. Homann, "Der Einfluss grosser Zahigkeit bei der Strommung um den Zylinder und um die Kugel", Zietsche. f. angew. Math. u. Mech. (1936), pp. 153-164; especially pp. 155-159.

(5) Iadenberg, Winckler and Van Voorhis, "Interferometer Studies of Faster than Sound phenomona", The Physical Review, Vol. 73, No. 11, June 1,(1948).

(6) H. W. Liepmann and A. E. Puckett, "Aerodynamics of a Compressible Fluid", John Wiley and Sons, 1946.

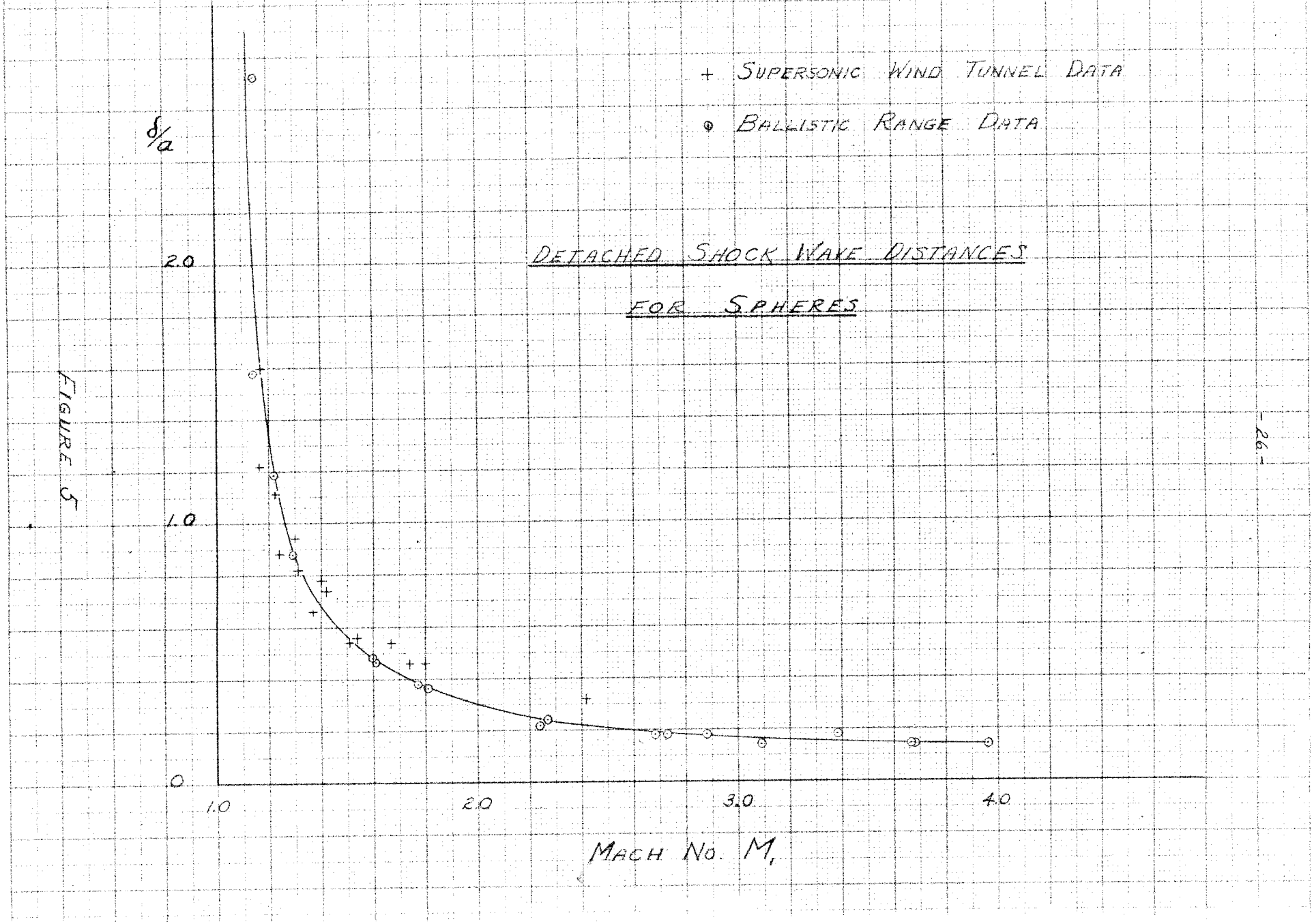

DETACHED SHOCK WAKE DISTANCES FOR SPHERES

FIGURE 5

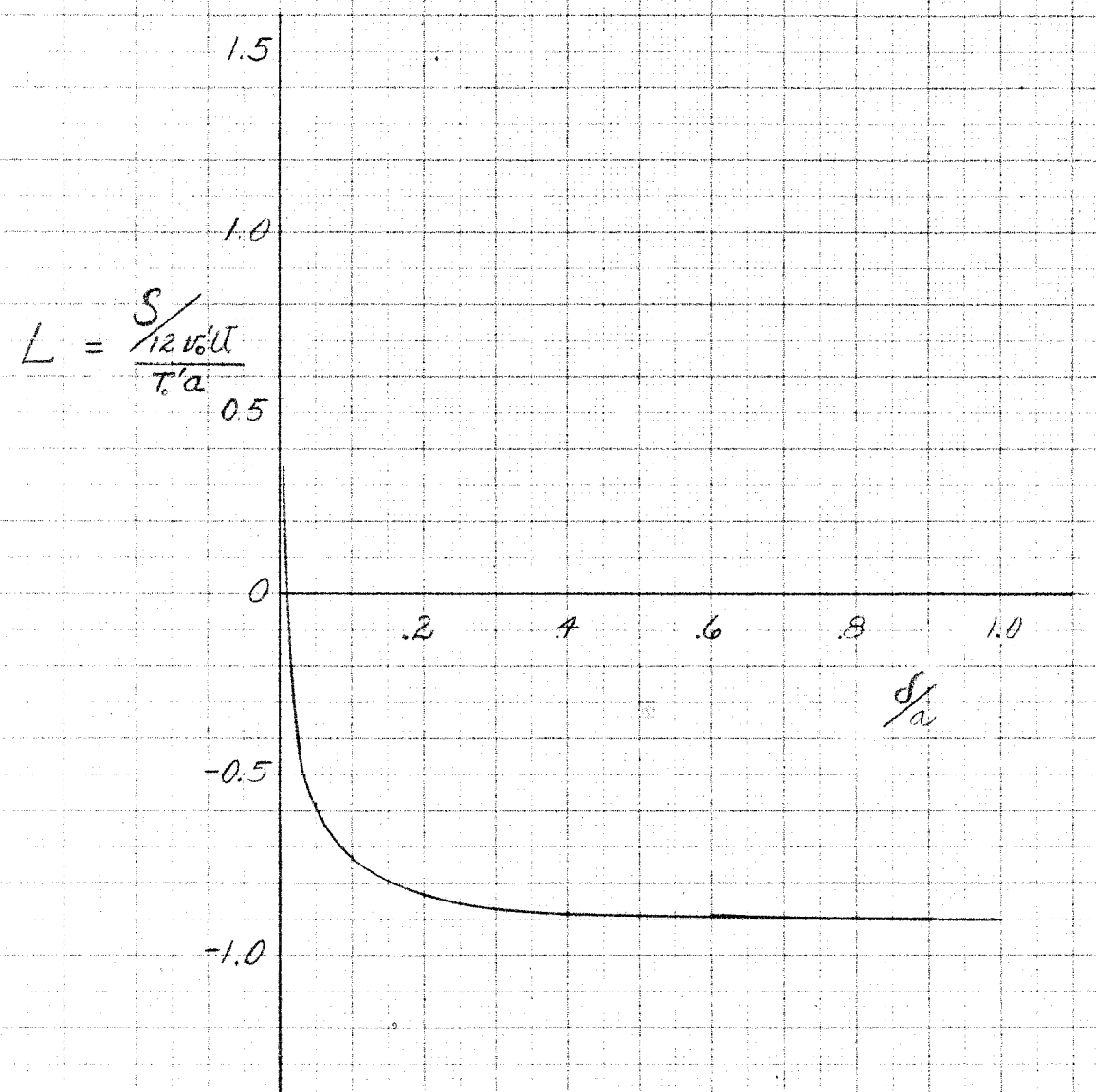

PARAMETRIC VALUE OF ENTROPY RISE THROUGH POTENTIAL TYPE FLOW REGION

FIGURE 6

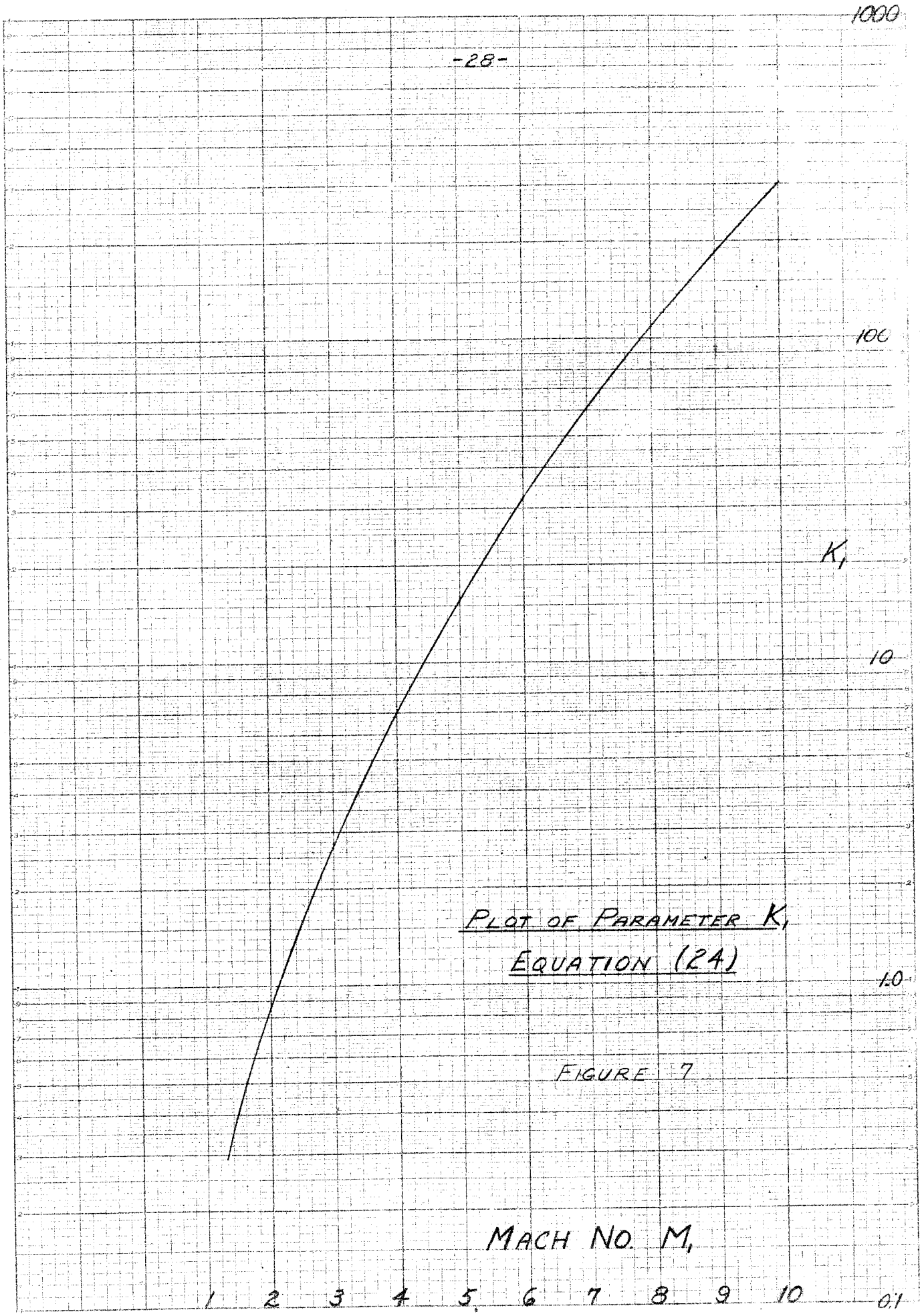

PLOT OF PARAMETER K_1
EQUATION (24)

FIGURE 7

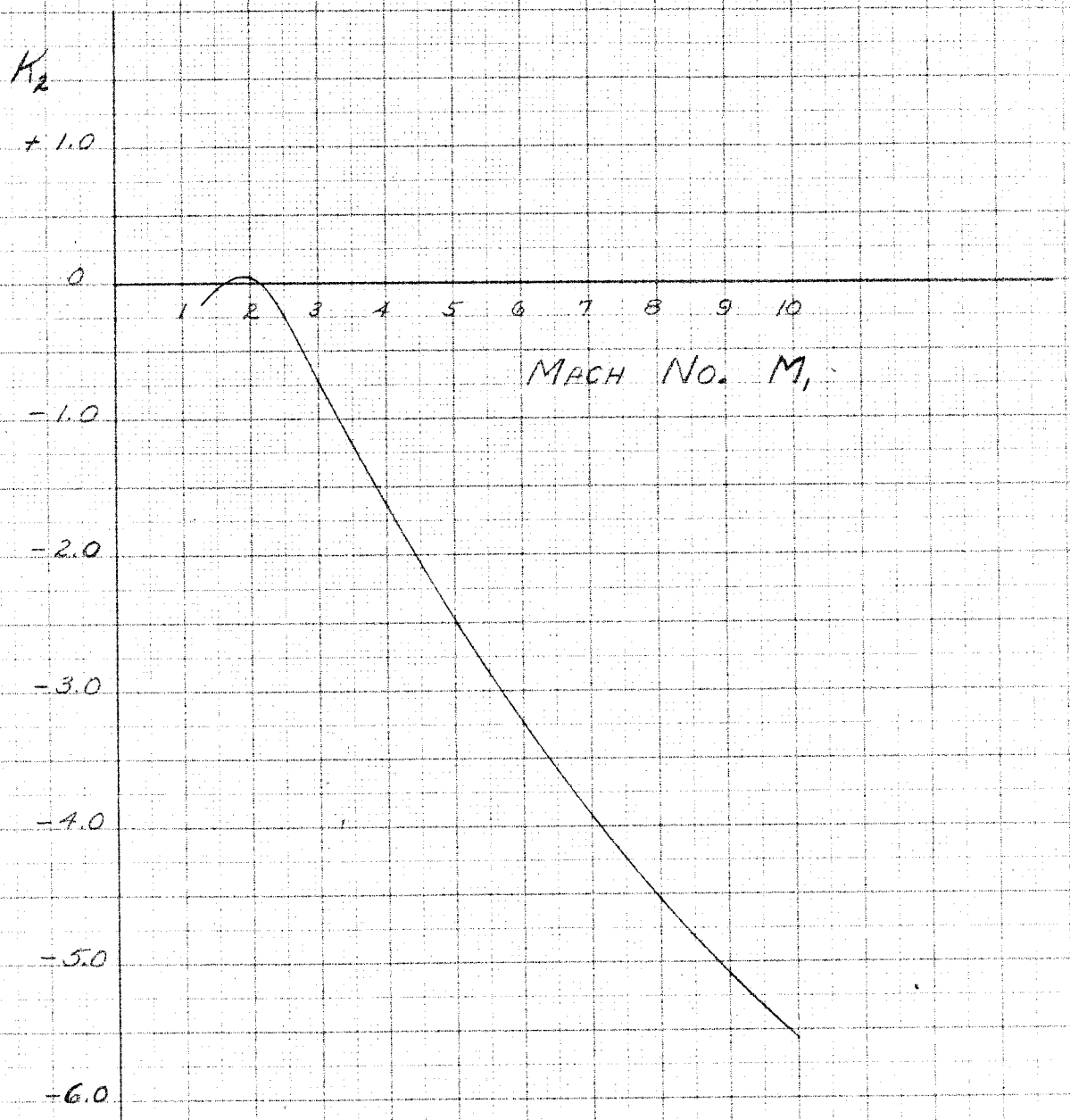

PLOT OF PARAMETER K_2

EQUATION (25)

FIGURE 8

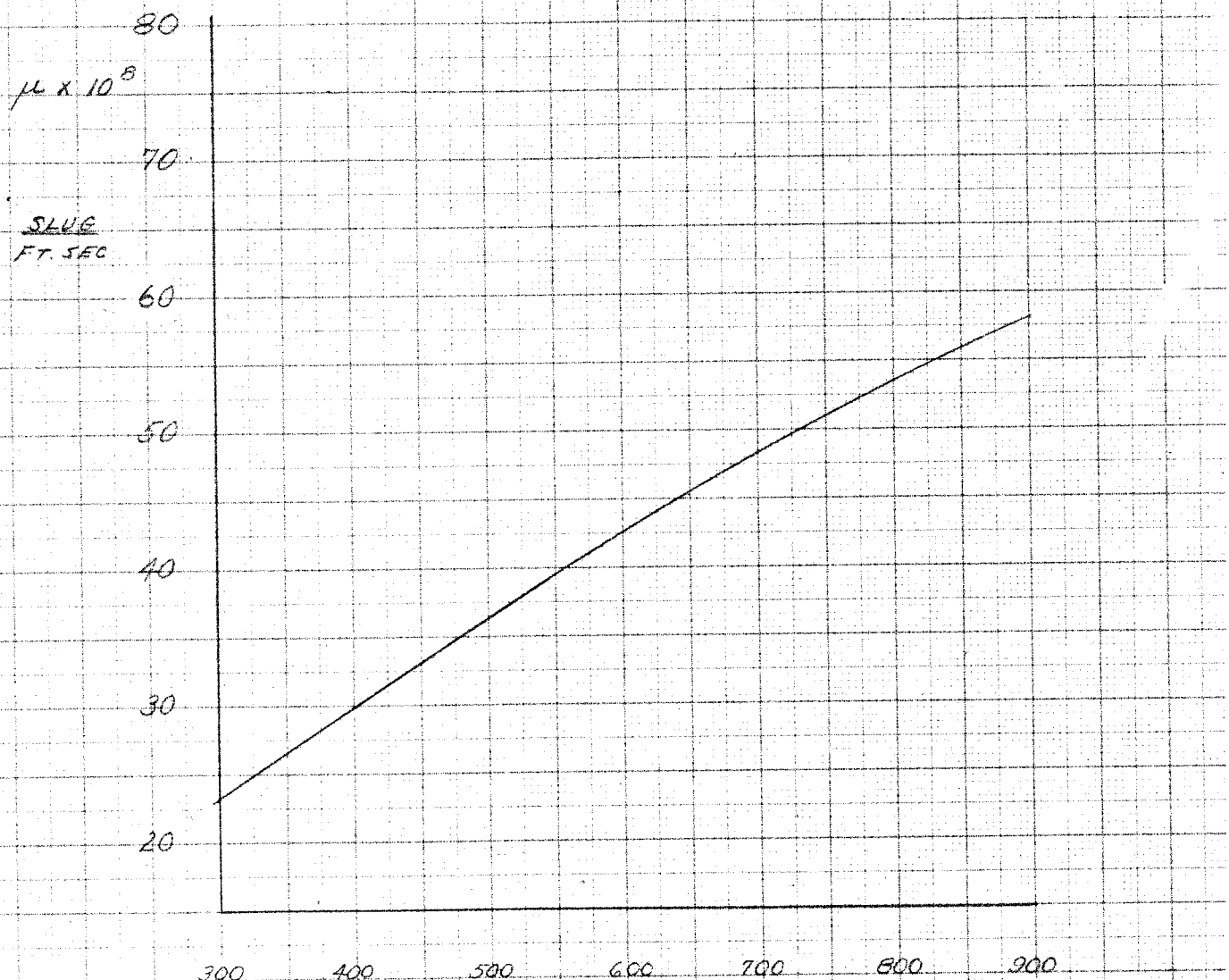

VISCOSITY OF AIR

FIGURE 9

APPENDIX A

BOUNDARY LAYER SOLUTION NEAR A FORWARD STAGNATION POINT

BOUNDARY LAYER SOLUTION NEAR A FORWARD STAGNATION POINT

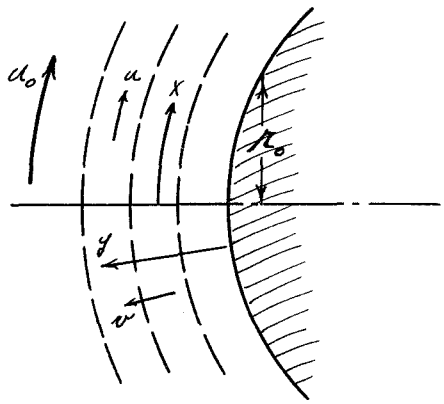

Figure 1A

Description of Coordinates for Boundary Layer Problem

The equation of continuity, in curvilinear orthogonal coordinates possessing one axis of symmetry can be written

$$\frac{1}{r}\left[\frac{\partial}{\partial x}(ru) + \frac{\partial}{\partial y}(rv)\right] = 0$$

where x, y are coordinates as indicated above. Since $r \cong r_o \cong x$ in the vicinity of the stagnation point, the equation of continuity becomes

$$\frac{\partial}{\partial x}(xu) + \frac{\partial}{\partial y}(xv) = 0$$

This equation implies a stream function ψ such that

$$u = \frac{1}{x}\frac{\partial \psi}{\partial y}$$

$$v = -\frac{1}{x}\frac{\partial \psi}{\partial x}$$

which identically satisfies the continuity equation.

The equations of motion in two dimensions are

$$u\frac{\partial u}{\partial x} + v\frac{\partial u}{\partial y} = -\frac{1}{\rho}\frac{\partial p}{\partial x} + \nu\frac{\partial^2 u}{\partial y^2} + \nu\frac{\partial^2 u}{\partial x^2}$$

$$u\frac{\partial v}{\partial x} + v\frac{\partial v}{\partial y} = -\frac{1}{\rho}\frac{\partial p}{\partial y} + \nu\frac{\partial^2 v}{\partial x^2} + \nu\frac{\partial^2 v}{\partial y^2}$$

In the boundary layer, these equations reduce to

$$-\frac{1}{\rho}\frac{\partial p}{\partial y} = O(\delta) = 0$$

$$u\frac{\partial u}{\partial x} + v\frac{\partial u}{\partial y} = \frac{1}{\rho}\frac{\partial p}{\partial x} + \nu\frac{\partial^2 u}{\partial y^2}$$

by the method of establishing the equations, by Prandtl.

Since p is independent of y,

$$-\frac{1}{\rho}\frac{\partial p}{\partial x} = u_o\frac{du_o}{dx}$$

where u_o is the velocity outside the boundary layer. The momentum equation can then be written

$$u\frac{\partial u}{\partial x} + v\frac{\partial u}{\partial y} = u_o\frac{du_o}{dx} + \nu\frac{\partial^2 u}{\partial y^2}$$

Near the forward stagnation point the velocity u_o, just outside the boundary layer, may be put equal to βx, where x is the distance along meridian curve from the stagnation point.

Hence with

$$u = \frac{1}{x}\frac{\partial \psi}{\partial y}$$

$$v = -\frac{1}{x}\frac{\partial \psi}{\partial x}$$

$$u\frac{\partial u}{\partial x} + v\frac{\partial u}{\partial y} = \beta^2 x + \nu\frac{\partial^2 u}{\partial y^2}$$

a solution is obtained by putting

$$\eta = \left(\frac{\beta}{\nu}\right)^{\frac{1}{2}} y$$

$$\psi = (\beta\nu)^{\frac{1}{2}} x^2 f(\eta)$$

Thus

$$u = \beta x f'(\eta)$$

$$v = -2(\beta\nu)^{\frac{1}{2}} f(\eta)$$

$$\beta x f'(\eta)\beta f'(\eta) - 2(\beta\nu)^{\frac{1}{2}} f(\eta)\beta x f''(\eta)\left(\frac{\beta}{\nu}\right)^{\frac{1}{2}} = \beta^2 x + \beta^2 x f'''(\eta)$$

Calling $f(\eta) = f$, this equation reduces to

$$f'^2 - 2ff'' = 1 + f'''$$

Since

$$u = v = 0 \quad \text{at } y = 0$$

and

$$u = u_0 = \beta x \quad \text{at } y = \infty$$

the boundary conditions for f are

$$f(0) = 0$$

$$f'(0) = 0$$

$$f'(\infty) = 1$$

Choosing a solution for f of the form

$$f = \sum_{0}^{\infty} a_n \eta^n$$

then

$$f' = \sum_{0}^{\infty} n\, a_n \eta^{n-1}$$

$$f'' = \sum_{0}^{\infty} n(n-1)\, a_n \eta^{n-2}$$

$$f''' = \sum_{0}^{\infty} n(n-1)(n-2)\, a_n \eta^{n-3}$$

Substituting in the differential equation, and collecting coefficients of like powers of η, the values of a_n may be evaluated. The values for a_1 through a_8 as determined by Homann (Ref. 3) are

$$a_0 = 0$$

$$a_1 = 0$$

$$a_2 = \text{arbitrary}$$

$$a_3 = -0.16667$$

$$a_4 = 0$$

$$a_5 = 0$$

$$a_6 = 0.005556\, a_2$$

$$a_7 = -0.0003968$$

$$a_8 = 0$$

Thus

$$f = a_2 \eta^2 - 0.16667 \eta^3 + 0.005556 a_2 \eta^4 - 0.0003968 \eta^7 + \cdots$$

To determine a_2, from boundary condition

$$\eta = \infty \qquad f' = 1$$

let

$$f = f_0 + f_1$$

$$f' = f_0' + f_1'$$

$$f_0' = 1 \ , \quad f_1' = 0 \quad \text{at } \eta = \infty$$

Thus

$$f = \eta + f_1$$

Substituting in original differential equation,

$$(1 + f_1')^2 - 2(\eta + f_1) f_1'' = 1 + f_1'''$$

$$2 f_1' + f_1'^2 - 2\eta f_1'' - 2 f_1 f_1'' = f_1'''$$

neglecting f_1 and $f_1'^2$ in comparison with the other terms

$$f_1''' + 2\eta f_1'' - 2 f_1' = 0$$

This equation has the solution

$$f_1' = A_1 \eta \int_{\infty}^{\eta} \frac{1}{\tau^2} e^{-\tau^2} d\tau$$

$$f_1 = A_2 + \int_0^\eta A_1 \eta \int_\infty^\eta \frac{1}{\tau^2} e^{-\tau^2} d\tau \, d\eta$$

$$f_1 = A_2 - A_1 \int_0^\eta e^{-\tau^2} d\tau - 2A_1 \int_0^\eta \tau \, d\tau \int_\infty^\tau e^{-u^2} du$$

From Homann, $A_1 = 2.16492$, $A_2 = -0.557611$ and $a_2 = 0.658619$, determined by equating

$$f = \sum_0^\infty a_n \eta^n = \eta + f_1$$

Thus

$$\begin{aligned} a_0 &= 0 \\ a_1 &= 0 \\ a_2 &= +0.658619 \\ a_3 &= -0.16667 \\ a_4 &= 0 \\ a_5 &= 0 \\ a_6 &= 0.00366 \\ a_7 &= -0.0003968 \\ a_8 &= 0 \end{aligned}$$

The final expression for f is then

$$f = 0.6586\eta^2 - 0.16667\eta^3 + 0.00366\eta^6 - 0.00040\eta^7 + \cdots$$

and is graphically represented, together with f' and $\frac{f'^2}{f}$, in Figure 2A.

From the definitions for u and v given above, these velocities may be written

$$u = 1.3172\,\beta\left(\frac{\beta}{\nu}\right)^{\frac{1}{2}} xy - 5.000\,\frac{\beta^2}{\nu}\,xy^2$$

$$v = -1.3172\,\beta\left(\frac{\beta}{\nu}\right)^{\frac{1}{2}} y^2 + 0.3333\,\frac{\beta^2}{\nu}\,y^3$$

where only two terms of the series expansion for f are employed.

The notation used in this appendix is standard boundary layer nomenclature, and differs from that used in the main body of this thesis. For use there, the two equations above for u and v are then written as

$$u = -1.3172\,\beta\left(\frac{\beta}{\nu}\right)^{\frac{1}{2}} x^2 + 0.3333\,\frac{\beta^2}{\nu}\,x^3$$

$$v = 1.3172\,\beta\left(\frac{\beta}{\nu}\right)^{\frac{1}{2}} xy - 0.5000\,\frac{\beta^2}{\nu}\,yx^2$$

GRAPHICAL REPRESENTATION

SOLUTION OF

BOUNDARY LAYER PROBLEM

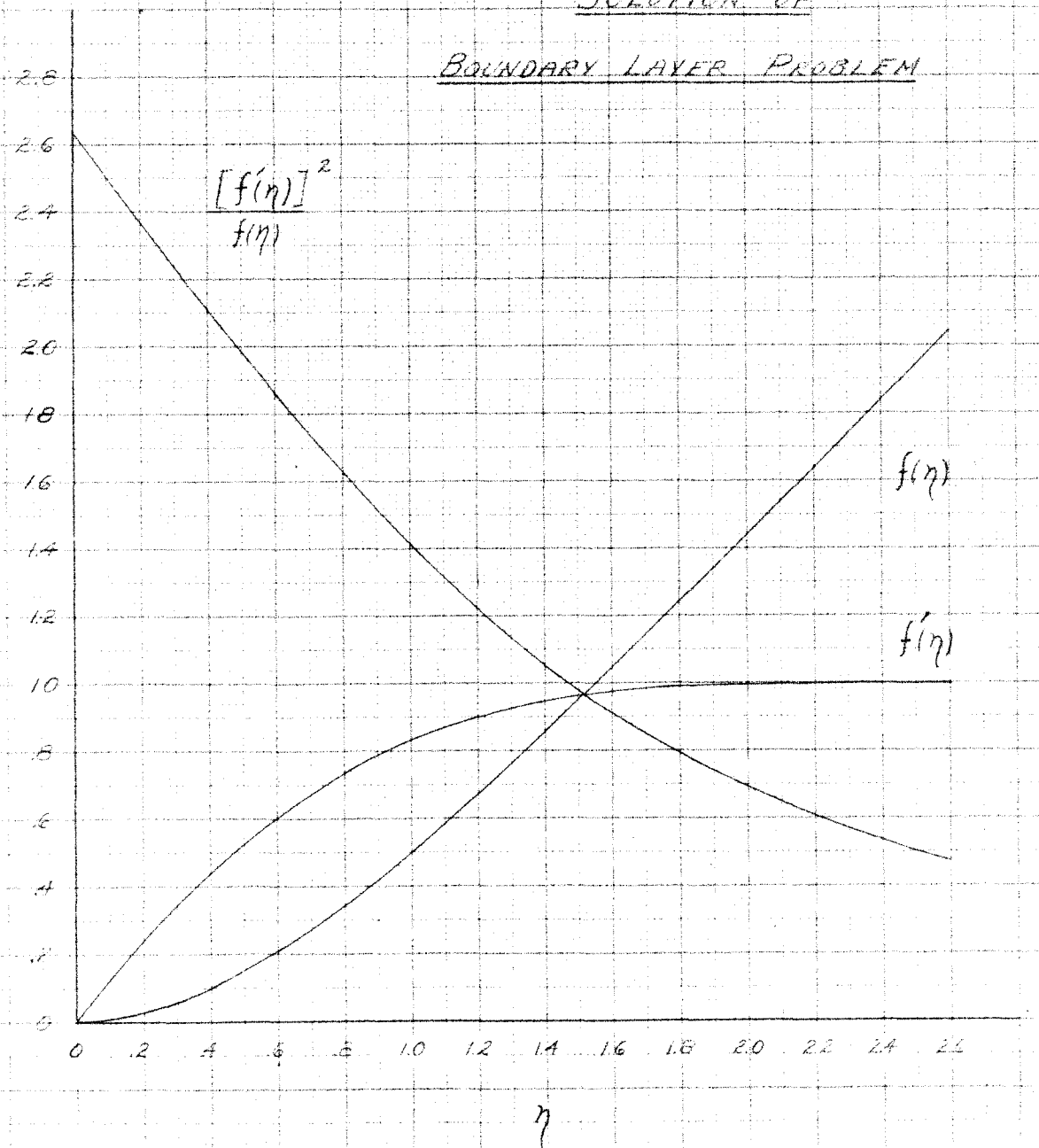

FIGURE 2A

APPENDIX B

GRAPHICAL SOLUTION FROM DATA OBTAINED FROM AN INTERFEROMETER STUDY OF DETACHED SHOCK WAVES

GRAPHICAL SOLUTION FROM DATA OBTAINED FROM AN INTERFEROMETER STUDY OF DETACHED SHOCK WAVES

Figure 24 of Reference 5, reproduced here in part as Figure 1B, is an isopycnal chart for air flow about a sphere in a supersonic jet of Mach number 1.70. In this chart the contours are labeled in milligrams per cubic centimeters. These data were computed from an interferogram of air flow about a 9/32 inch diameter sphere in a homogeneous jet.

Figure 2B is a plot of the density against distance along the axis of symmetry, taken from Figure 1B.

The equations used for the determination of the pressure p_2, the temperature T_2, and the velocity u_2, as given in Reference (5), are

$$p_2 = 0.414\, \rho_2^{\gamma} \quad \text{atmos}$$

$$T_2 = 144\, \rho_2^{\gamma-1} \quad {}^{\circ}\text{Kelvin}$$

$$u_2 = 533\, (2.063 - \rho_2^{\gamma-1})^{\frac{1}{2}} \quad \text{meters/sec.}$$

Using the plotted values of the density, the temperatures and the velocities may be determined conveniently from these relations. The variation of the temperature and the velocity along the axis of symmetry is graphically represented in Figures 3B and 4B. Figure 3B and Figure 4B

are actually the same plot; however, in Figure 45 the state parameters which are necessary for a stepwise integration have been more smoothly faired, and have been expressed in more convenient units.

From Equation (8)

$$\Delta S = \frac{4}{3}\frac{\nu_2}{T_2}\int_{\delta}^{0}\frac{1}{u_2}\left(\frac{du_2}{dx}\right)^2 dx$$

and using the values of density, temperature, and velocity plotted in Figure 45, a stepwise integration was performed, and the entropy rise along the axis of symmetry was determined. For this computation, the value of μ was fixed at 3.7×10^{-8} slugs/ft.sec. This procedure then gives

$$\Delta S = 0.086 \quad ft^2/sec^2\ ^\circ Rankine$$

$$p_o'/p_o'' = 1.000050$$

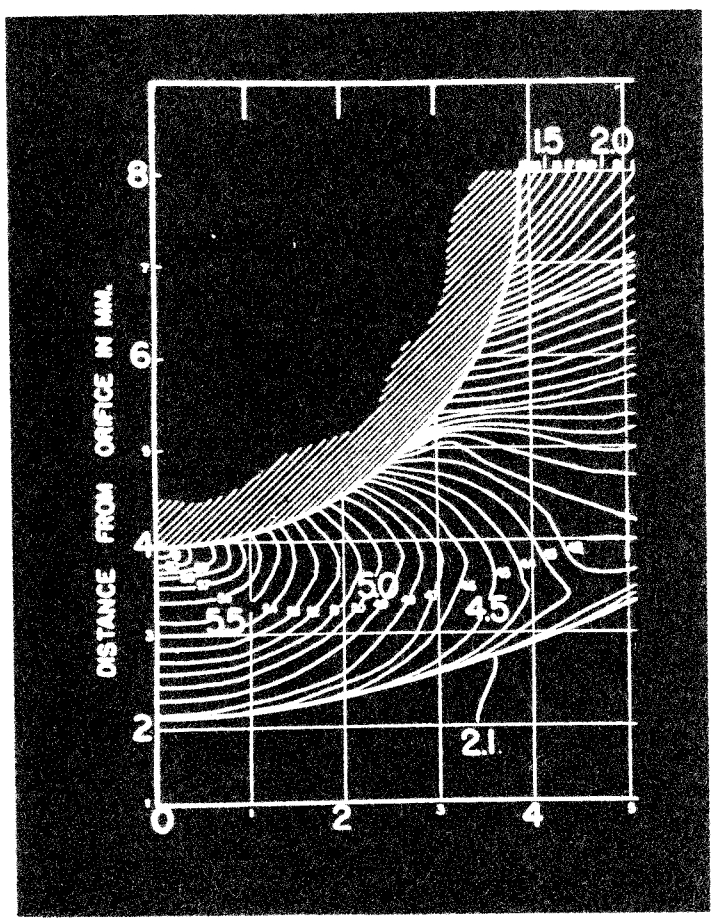

ISOPYCNAL CHART

FOR AIR FLOW AROUND A SPHERE

FROM INTERFEROMETER STUDY

$M = 1.70$

FIGURE 1B

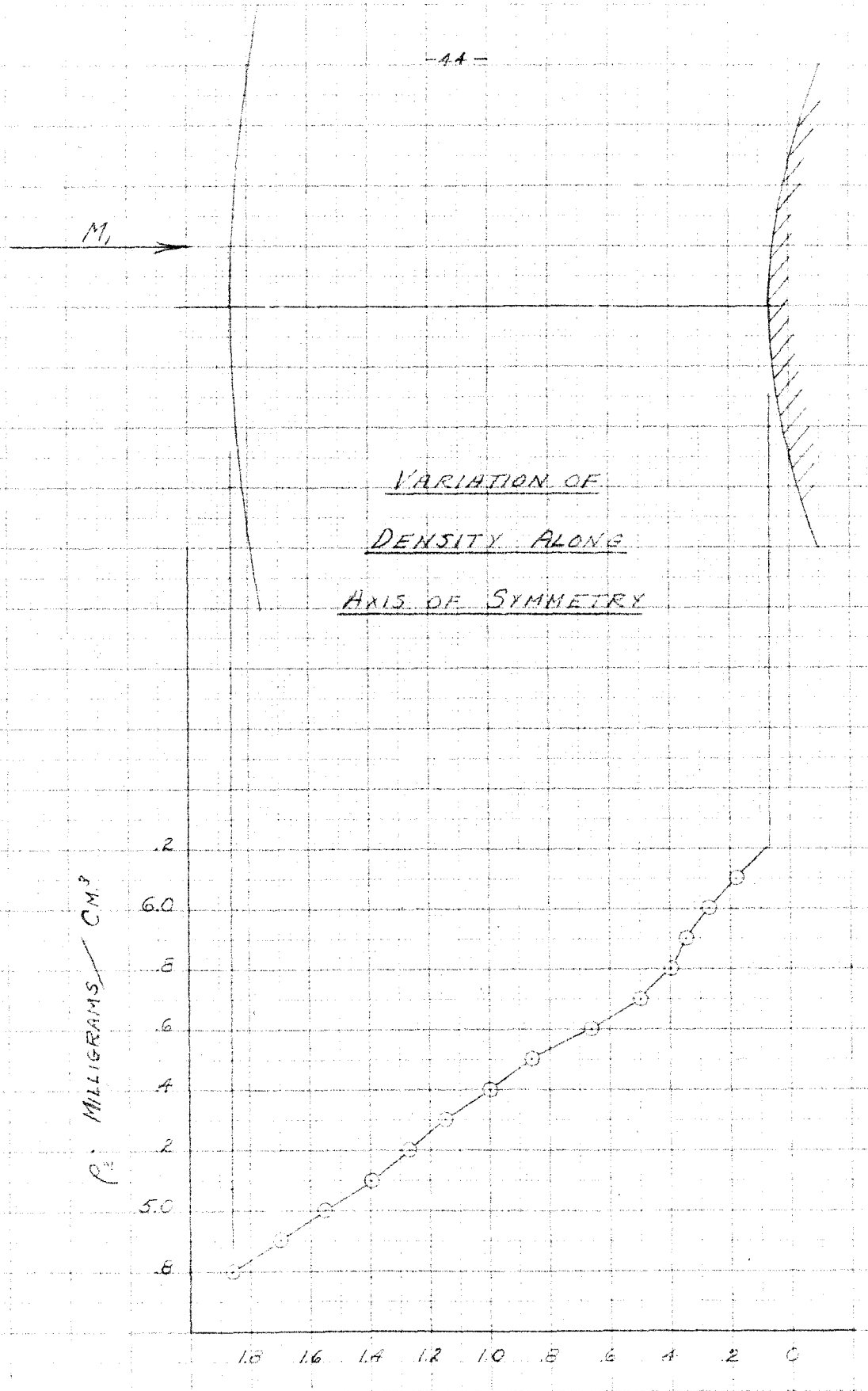
M1
VARIATION OF
DENSITY ALONG
AXIS OF SYMMETRY
ρ - MILLIGRAMS / CM.³
.2
6.0
.8
.6
.4
.2
5.0
.8
1.8
1.6
1.4
1.2
1.0
.8
.6
.4
.2
0
DISTANCE IN MILLIMETERS
ALONG AXIS OF SYMMETRY

FIGURE 2B

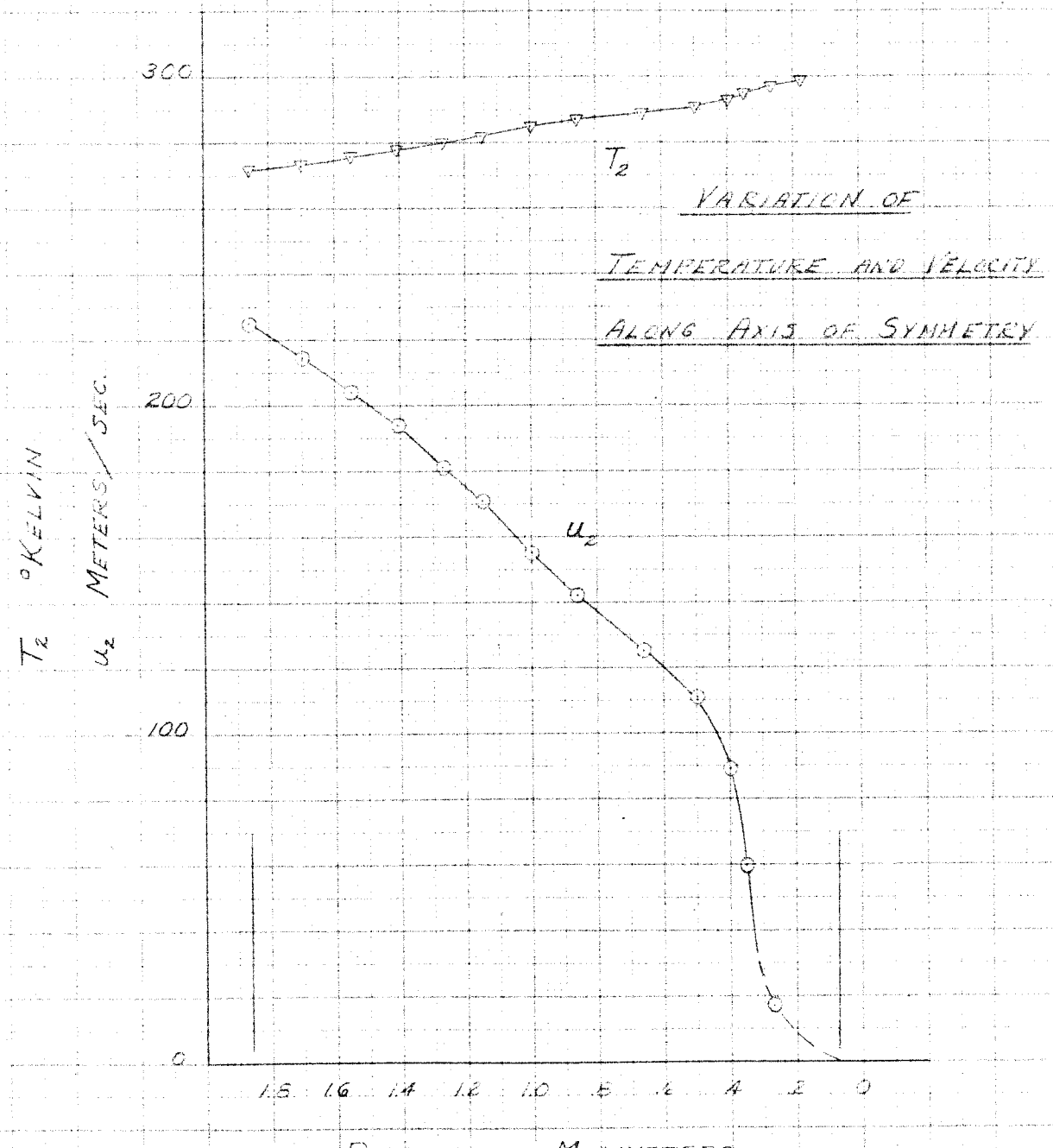
300
200
100
0
T_2
u_2
VARIATION OF
TEMPERATURE AND VELOCITY
ALONG AXIS OF SYMMETRY
T_2 °KELVIN
u_2 METERS/SEC.
1.8 1.6 1.4 1.2 1.0 .8 .6 .4 .2 0
DISTANCE IN MILLIMETERS
ALONG AXIS OF SYMMETRY

FIGURE 3B

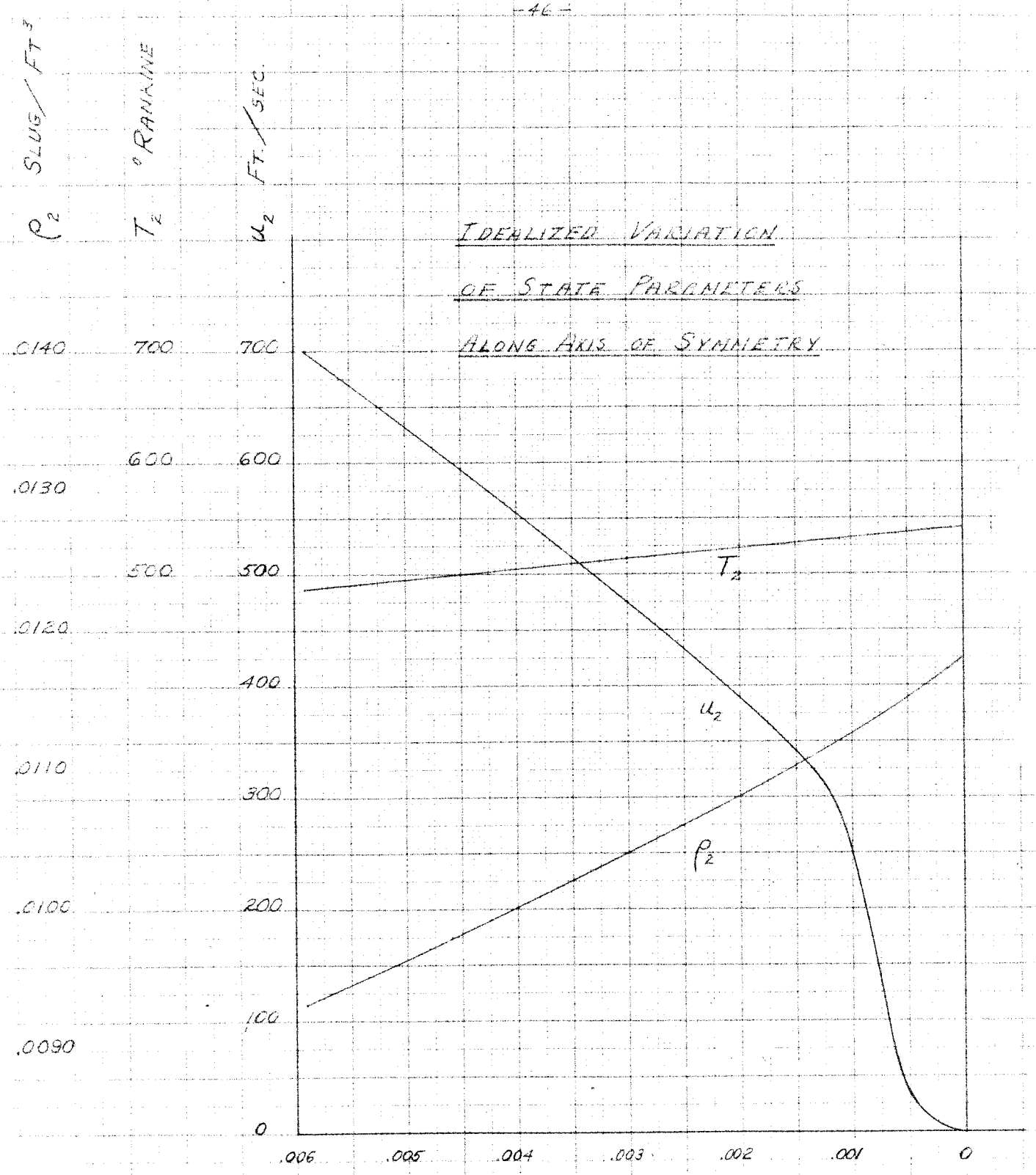
IDEALIZED VARIATION
OF STATE PARAMETERS
ALONG AXIS OF SYMMETRY
ρ_2 SLUG/FT^3
T_2 °RANKINE
u_2 FT./SEC.
.0140
.0130
.0120
.0110
.0100
.0090
700
600
500
400
300
200
100
0
.006
.005
.004
.003
.002
.001
0
T_2
u_2
ρ_2
DISTANCE IN FEET
ALONG AXIS OF SYMMETRY

FIGURE 48